Z-pinch Driven Inertial Confinement Fusion Target Physics Research at Sandia National Laboratories*

R. J. Leeper, T. E. Alberts, J. R. Asay, P. M. Baca, K. L. Baker, S. P. Breeze, G. A. Chandler, D. L. Cook, G. W. Cooper, C. Deeney, M. S. Derzon, M. R. Douglas, D. L. Fehl, T. Gilliland, D. E. Hebron, M. J. Hurst, D. O. Jobe, J. W. Kellogg, J. S. Lash, S. E. Lazier, M. K. Matzen, T. A. Mehlhorn, D. H. McDaniel, J. S. McGurn, A. R. Moats, R. C. Mock, D. J. Muron, T. J. Nash, R. E. Olson, J. L. Porter, J. P. Quintenz, P. V. Reyes, L. E. Ruggles, C. L. Ruiz, F. A. Schmidlapp, J. F. Seamen, R. B. Spielman, T. W. L. Sanford, M. A. Stark, K. W. Struve, W. A. Stygar, D. R. Tibbetts-Russell, J. A. Torres, M. Vargas, T. C. Wagoner, and C. Wakefield

Sandia National Laboratories, Albuquerque, New Mexico USA

J. H. Hammer, D. D. Ryutov, M. Tabak, and S. C. Wilks

Lawrence Livermore National Laboratory, Livermore, California USA

R. L. Bowers, K. D. McLenithan, and D. L. Peterson

Los Alamos National Laboratory, Los Alamos, New Mexico USA

Abstract

Three hohlraum concepts are being pursued at Sandia National Laboratories (SNL) to investigate the possibility of using pulsed power driven magnetic implosions (z-pinches) to drive high gain targets capable of yields in the range of 200-1000 MJ. This research is being conducted on SNL's Z facility that is capable of driving peak currents of 20 MA in z-pinch loads producing implosion velocities as high as $7.5X10^7$ cm/s, x-ray energies approaching 2 MJ, and x-ray powers exceeding 200 TW. This paper will discuss each of these hohlraum concepts and will overview the experiments that have been conducted on these systems to date.

1.0 INTRODUCTION

The U. S. Department of Energy is supporting research at Sandia National Laboratories (SNL) to investigate the possibility of using pulsed power driven magnetic implosions (z-pinches) to drive high gain targets capable of yields in the range of 200-1000 MJ. This approach to inertial fusion energy provides an alternate and complementary technology to the laser-based approaches that are currently emphasizing target ignition and modest gain on facilities such as Omega and Nova in preparation for future experiments on the National Ignition Facility. Currently, the SNL program is pursuing three different concepts aimed at high yield from z-pinch sources. All of these concepts employ DT cryogenic capsules (2-4 mm in diameter) that are indirectly driven by radiation fields that are generated by z-pinch hohlraum radiation sources. Each of these three approaches to inertial fusion is similar in concept to the indirect laser approach to ICF [1].

Z-pinches have long fascinated the plasma physics community. In this geometrically-simple configuration it seemed easy to create high density and high temperature plasmas, perhaps reaching fusion conditions. However, extensive experimental and theoretical work in the 1950's and 1960's, an example of which is cited as Reference [2], indicated that magneto-hydrodynamic instabilities prevented the pinched plasmas from reaching the required plasma temperatures and densities for fusion in equilibrium. During the 1980's, there was a short revival in interest in z-pinch-driven fusion due to the new capability to make cryogenic fibers [3]. Recently, improvements in the technology of fast pulsed electrical power have re-opened interest in the field of fast, dynamic z-pinches as x-ray sources for indirect-drive Inertial Confinement Fusion

* Sandia is a multiprogram laboratory operated by Sandia Corporation, a Lockheed Martin Company, for the United States Department of Energy under Contract DE-AC04-94AL85000.

(ICF) applications [4-5]. The word "fast" in this context refers to a class of z-pinches where a submicrosecond electrical pulse (~100 ns current rise time on the Z accelerator) implodes an annular, cylindrically symmetric plasma at supersonic velocities. These supersonic implosions are in contrast to the classic fusion pinches which were usually designed to achieve a Bennett equilibrium. In fast z-pinches, the azimuthal magnetic field associated with the axial flow of a large current through the cylindrically symmetric plasma creates a magnetic pressure (J X B or Lorenz force) that accelerates the plasma radially inward. At the Z pulsed power accelerator at Sandia National Laboratories [6-7], currents of 20 MA flow through centimeter-size "z-pinch" plasmas, accelerating them to implosion velocities as high as 7.5×10^7 cm/s (i.e. Mach 10 to 20). The hot, dense plasma that is generated when this imploding plasma either stagnates and thermalizes at the cylindrical axis of symmetry or stagnates on a separate central cylindrical target is an efficient source of soft x-ray radiation.

In order to reach ignition and high yield (>200 MJ) with ICF capsules, strict requirements are placed on the radiation source, as has been reviewed by Lindl for laser-driven ICF [1]. Calculations show that the integrated radiation flux at the capsule ablation surface must be symmetric to within 1-2%, the absorbed x-ray energy must be greater than ~1 MJ, and the peak radiation flux must be greater than the equivalent of a 225 eV blackbody. In addition, the radiation pulse must have a precisely shaped and reproducible temporal profile. If the absorption efficiency (energy absorbed in the capsule ablator relative to total x-ray energy produced by the driver) is 10% within an ICF target configuration, then the x-ray source must provide on the order of 10 MJ. The high x-ray production efficiency of fast z-pinches make them attractive sources for testing ICF capsule concepts.

The first indirect-drive ICF target configuration being pursued at SNL, in collaboration with Los Alamos National Laboratory, is illustrated schematically in Fig. 1 [4]. This configuration is described as the dynamic, or imploding liner, hohlraum concept in which the imploding high-z plasma also serves as the hohlraum wall. This concept is the leading candidate for producing the highest temperatures with a z-pinch load [8-10]. In this system, the high yield ICF capsule is placed at the center of the smaller low-density foam structure on the cylindrical symmetry axis of the tungsten z-pinch imploding wire array. The radiation produced when the imploding plasma strikes the low-density foam quickly penetrates the low-density material and begins to ablate the ICF capsule. The stagnation of the imploding plasma and subsequent compression of the central

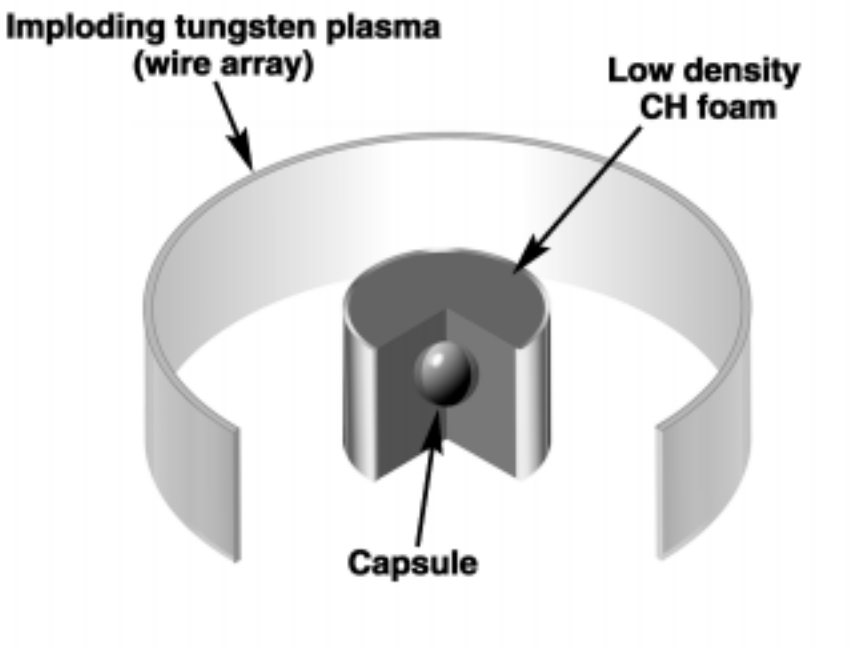

Fig. 1 Schematic of dynamic hohlraum concept.

cylinder results in a high temperature radiation drive in the interior of the foam. The low-density foam and the material that is ablated from the ICF capsule isolate the capsule ablation surface from the hydrodynamics of the imploding plasma; this creates a region in which the radiation mean-free-path is long, allowing a uniform radiation drive at the ablation surface. At a current level of 60 MA, George Allshouse designed a capsule within a dynamic hohlraum configuration that produced over 600 MJ of fusion yield [11].

Several physics issues must be addressed in order to experimentally validate the dynamic hohlraum target concept. The hydromagnetic Rayleigh-Taylor (RT) instability can break-up the imploding high-atomic-number z-pinch plasma (the hohlraum wall), permitting excessive loss of x-ray energy and large perturbations of the symmetry of x-ray drive on the fusion capsule due to spatial inhomogeneities in the hohlraum wall. When the imploding high-z plasma stagnates on the central low-z cylinder, mixing of these two materials may occur. Since the hohlraum wall material is necessarily very opaque, this mixing could affect the transport of x-rays to the capsule. To reach the high degree of implosion symmetry required in order to achieve the fusion capsule compression needed for ignition and high yield [1], the outward motion of the fusion capsule ablator material must hydrodynamically isolate the imploding spherical ablation surface of the fusion capsule from the imploding z-pinch hohlraum. Additionally, capsule implosions require a proper radiation pulse shape and low preheat to efficiently compress the fuel on a low adiabat.

A second indirect-drive ICF concept, termed static-walled hohlraum, being investigated at SNL, is shown in Fig. 2 [12]. In this concept, the ICF capsule is isolated from the x-ray generation region. Advantages in the areas of capsule drive symmetry and diagnostic access might be gained from this arrangement. Also, the hohlraum dimensions and z-pinch dimensions can be independently optimized in this type of arrangement. In this concept, x-rays from the z-pinch source enter the hohlraum through radiation entrance holes (REHs) on either end of the hohlraum. Since the source region outside of each REH is necessarily hotter than the interior of the hohlraum, symmetry shields are placed in a manner similar to heavy ion ICF concepts so as to

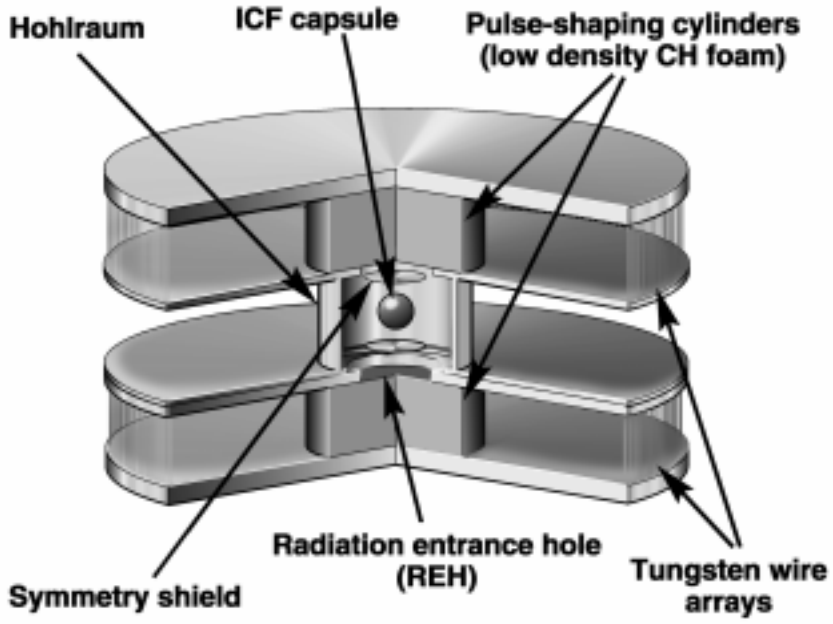

Fig. 2 Schematic of the z-pinch driven static-walled hohlraum ICF concept.

assure that the capsule is not driven in an excessively “pole hot” manner. In order to achieve adequate implosion symmetry, the hohlraum walls are placed at a radius that is about three times the capsule radius. The two wire arrays are initially located at a diameter of ~40-50 mm. Each

wire array is ~10 mm long and driven with currents ~50-60 MA. As the current rises, the tungsten wires are ohmically heated into a ~20-40 eV plasma state and are accelerated radially inward by the rising magnetic field pressure. The "pulse-shaping cylinder" has a diameter of ~6-12 mm. When the incoming tungsten plasma strikes the cylinder, the interior surface of the cylinder is heated to ~100 eV. The x-ray radiation from this moderately hot interior flows through the low-z foam or helium fill and heats the interior of the ICF hohlraum to the ~70-90 eV level. This process provides the 10-20 ns long "foot pulse" that is necessary to provide the initial shocks of ~1 Mb that are required to provide initial compression of the cryogenic DT fuel layer. Meanwhile, the combined mass of the wire array and cylinder wall continues to implode and provides a high intensity "peak pulse" of x-ray input as it stagnates on-axis. The x-ray input from the peak pulse must be ~300-600 TW in order to heat the hohlraum to the peak radiation temperature of ~250 eV that is required to achieve the final implosion velocity necessary for ICF ignition.

We envision that the combined central assembly containing the capsule, hohlraum, and central cylinders will be filled with low-density helium gas and/or CH foam and will be kept at a controlled cryogenic temperature of ~17-19 degrees K such that a uniform β-layering of the DT layer can be accomplished on the inner surface of the spherical ablator shell. We envision that the independent optimization of the cryogenic hohlraum and the z-pinch array could provide flexibility in progressing from NIF-scale ignition capsules to larger, higher-yield capsules of up to ~4 mm in diameter. The small X-1 hohlraums would be compatible in size and peak temperature with NIF-scale capsules. The larger X-1 hohlraum sizes would be used for larger capsules driven with longer pulse shapes and lower peak radiation temperatures. The basic idea is that the cryogenic assembly, hohlraum diameter, hohlraum temperature, pulse shape, and capsule could change markedly from one experiment to the next, while the z-pinch and MITL feed system might remain little changed in its radius, inductance, or electrical pulse length characteristics. Thus, we would be able to maintain an optimal, low inductance wire-array load regardless of the static-walled hohlraum dimensions. Preliminary experimental investigations of static-walled hohlraum temperature, diagnostic hole closure, axial temperature gradients, azimuthal symmetry, plasma filling, and x-ray shield/capsule configurations are currently underway on the Z facility.

The third indirect-drive ICF configuration that is being pursued in collaboration with Lawrence Livermore National Laboratory is illustrated schematically in Fig. 3 [13]. In this ICF concept, denoted z-pinch driven hohlraum, two cylindrical wire arrays are imploded in two primary radiation cavities located at either end of a capsule-containing central hohlraum. Enclosing each z-pinch in a high-z lined radiation cavity increases the x-ray power in the cavity by approximately $1/(1-\alpha)$ where α is the wall albedo. The albedo of high-z walls can typically be ~0.8, implying that the radiation power enhancement in each radiation cavity can be ~5. The thermal x-ray radiation produced by each z-pinch is then allowed to flow into the central hohlraum through wire mesh electrodes that are located at each end of the central hohlraum. The thermal x-rays in the central hohlraum provide the x-ray drive to implode the capsule that is quite similar to the indirect-drive laser and heavy ion ICF hohlraum configurations. As in the static-walled hohlraum, the symmetry of the x-ray flux at the capsule surface can be tuned by the placement and the number of the symmetry shields within the central ICF capsule hohlraum and through varying the length and diameter of the hohlraum. Pulse shaping might be achieved with multiple concentric wire arrays or other structures internal to the z-pinch-driven hohlraum radiators. Initial target designs predict that from 13 to 18 MJ of x-rays in a 10 ns pulse would provide adequate power, energy, and symmetry to drive a fusion capsule located in a central hohlraum. The capsule can absorb 1-2 MJ of x-rays and produce >400 MJ of yield if the necessary pulse shaping can be obtained without a large energy penalty. Experiments on the Sandia Z facility to investigate the x-ray flux and temperature that can be produced in a single primary radiation cavity, similar to either the top or bottom cavities in Fig. 3, are currently being conducted.

2.0 DYNAMIC HOHLRAUM SYSTEM

The dynamic hohlraum concept has been investigated on the Z facility using the experimental configuration shown in Fig. 4 [14-16]. This configuration allows the exploration of most of the basic physics issues associated with the full concept shown in Fig. 1. In the Z

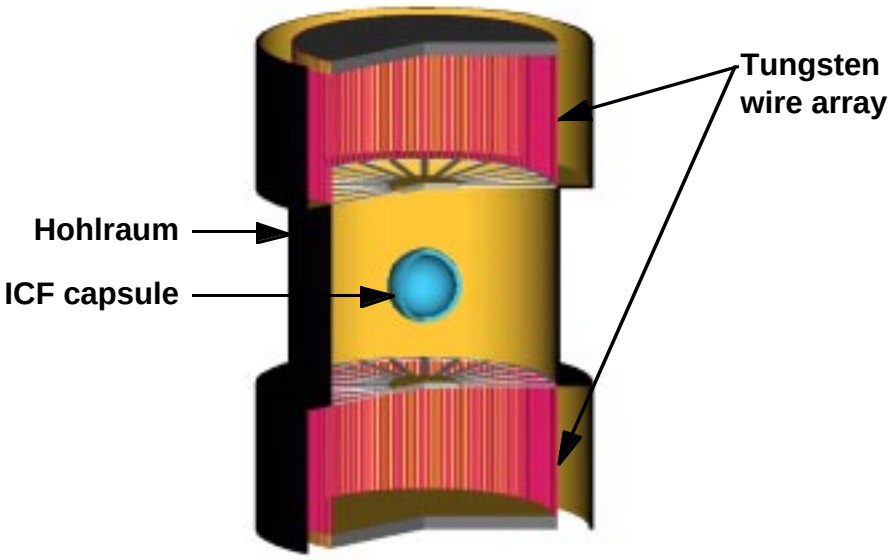

Fig. 3 Schematic of z-pinch driven hohlraum concept.

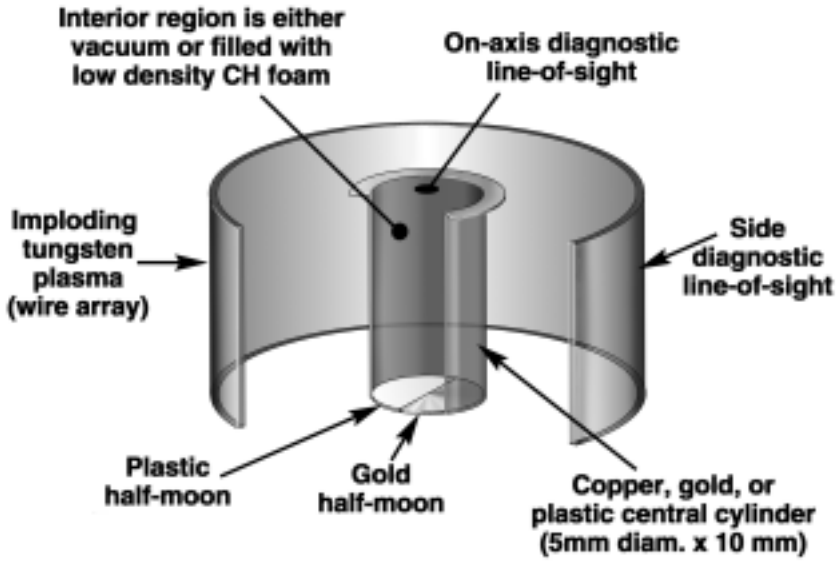

Fig. 4 Experimental arrangement used in dynamic hohlraum experiments.

experiments performed to date, the imploding tungsten wire array is made incident onto a central cylindrical gold, copper, or plastic target. The central target is typically 5 mm or 8 mm in diameter and 10 mm tall. The thickness varies from 0.5-2 μm for gold and copper targets to 16 μm for plastic targets. The interior region of the target is either vacuum or filled with low density (6 mg/cc to 14 mg/cc) CH foam. An axial soft x-ray diagnostic suite consisting of a bolometer array, an x-ray framing camera, and an x-ray diode array is used to observe radiation emission from the interior region of the target [17-18]. As shown in Fig. 4, a plastic half-moon and a gold half-moon are placed at the bottom of the target. The purpose of this arrangement is to insure that we are observing an optically thin system in the interior of the target by the measurement of the albedo contrast between the gold and plastic half-moons.

Data from a recent plastic target shot on the Z facility are shown in Figs. 5-7. This experimental configuration consisted of a nested, 1 cm long tungsten wire array that contained

240 wires at an initial diameter of 40 mm and 120 wires at an initial diameter of 20 mm. The total wire mass was 3 mg. The drive current in the tungsten wire array was 20.0 MA. This nested wire array was imploded onto a 5 mm diameter, 1 cm long solid density plastic annulus with a thickness of 16 μm and a total mass of 2.5 mg. A gold and plastic half-moon witness plate was

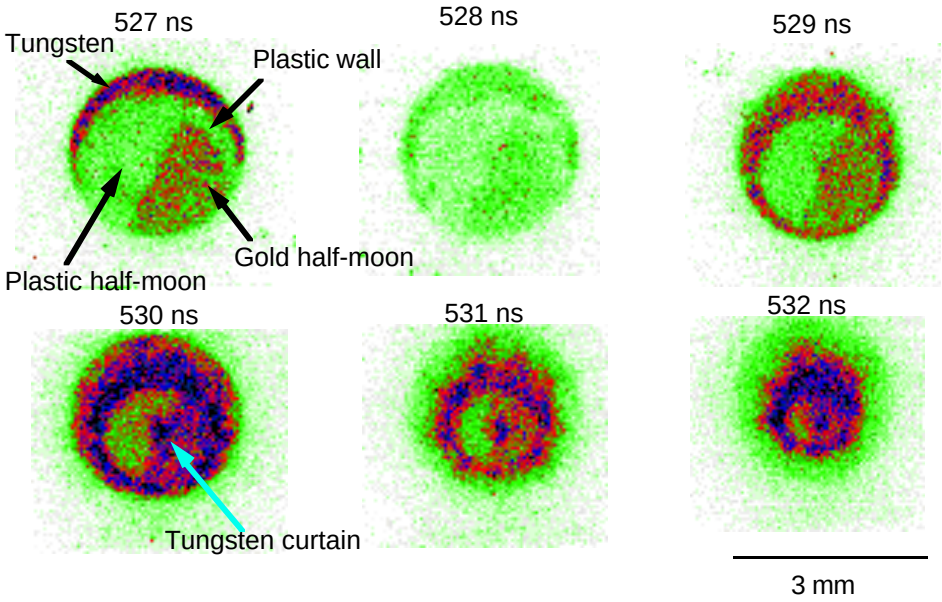

Fig. 5 Axial framing camera for plastic annulus target viewed from above at 6 degrees.

placed on the bottom of the target as described above. A framing camera viewed this target along its axis at angle of 6 degrees to the vertical. Eleven images of 1 ns dwell time were obtained for each of two energy cuts. Six frames of data from this camera that were obtained in an energy band of 250-280 eV are shown in Fig. 5. The time-dependent radial temperature profiles obtained from this data normalized to the x-ray flux measured with the bolometer array and x-ray diodes are shown in Fig. 6. Several important features are apparent in this data. First, the position of the tungsten wire array upon striking the target can be seen to move inward as a function of time. Second, the albedo contrast of the gold and plastic half-moon witness plate is clearly visible indicating that the interior region is optically thin to the soft x-ray radiation produced in its interior. Third, because of the small angle of the framing camera to the vertical, it was possible to observe the inside plastic wall of the target burnthrough and go into equilibrium with the plastic half-moon of the compressing system. Finally, starting in the 530 ns frame, a peak in temperature near center axis is observed that is attributed to a small amount of tungsten blowing across the top of the target and stagnating on axis. Fig. 7 shows the diameter of the tungsten sheath (defined as the centroid of the tungsten profile obtained from Fig. 5) versus time. The tungsten sheath had an implosion velocity of 35 cm/μs during the last 5 ns of the implosion. Also shown in Fig. 7 is the brightness temperature of the hohlraum as function of time. The increase in temperature as the diameter of system decreases clearly demonstrates the basic concept of a dynamic hohlraum. As can be seen from Fig. 7, a peak brightness temperature of 180 ± 15 eV was reached at 532 ns at a diameter of 1.6 mm. This temperature represents the approximate highest useful temperature for driving an ICF capsule since capsules designed to date for this system have diameters of 1.6 mm. As the system goes to smaller diameters (and higher temperatures), the tungsten would be incident onto the capsules and make large perturbations to its implosion. Although ablation from the capsule and the consequent retardation of the incoming system (ablation standoff) could help protect the capsule to some degree from these implosion perturbations, we have adopted a working definition of the brightness temperature for a dynamic hohlraum capsule system as the brightness temperature that is obtained when the tungsten sheath during its implosion reaches the capsule diameter (typically at 1.6 mm) being considered for the system.

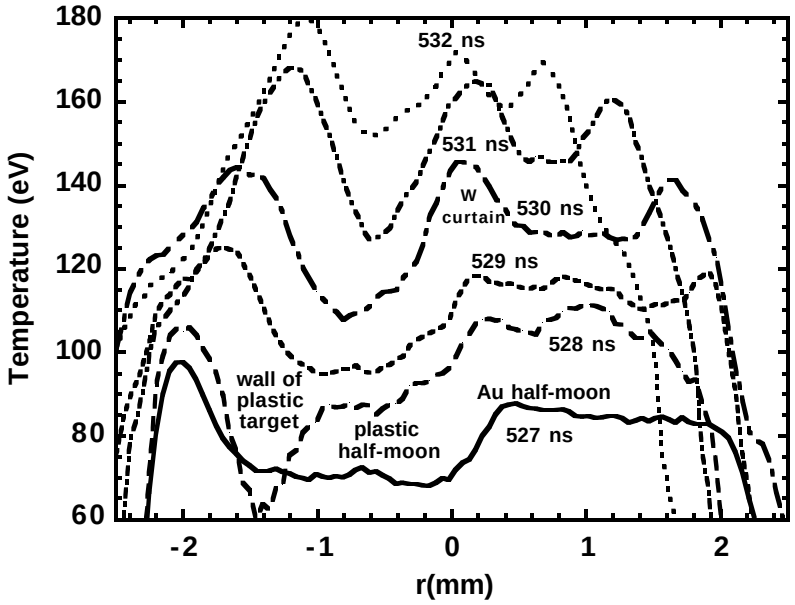

Fig. 6 Radial temperature profiles for plastic annulus target shot.

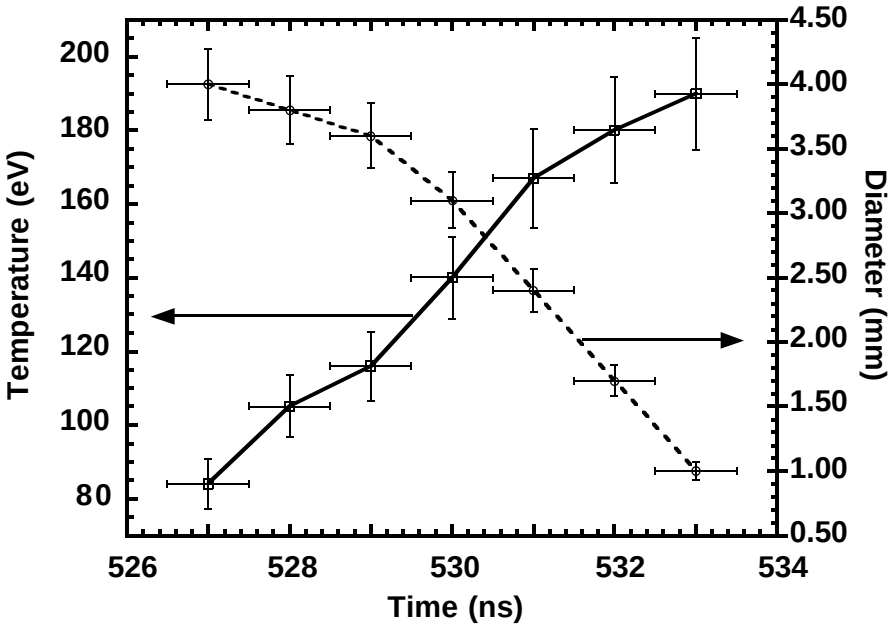

Fig. 7 Diameter and temperature versus time for plastic annulus target shot.

Data from a recent low density foam target on the Z facility are shown in Figs. 8-9. This experimental configuration consisted of a nested, 1 cm long tungsten wire array that contained 240 wires at an initial diameter of 40 mm and 120 wires at an initial diameter of 20 mm. The total wire mass was 3 mg. The drive current in tungsten wire array for this shot was 20.0 MA.

This nested wire array was imploded onto a 5 mm diameter, 1 cm long self-supporting 14 mg/cc CH plastic foam central target that had a total mass of 3.0 mg. This target did not have a high-z coating on its outside. A gold and plastic half-moon witness plate was placed on the bottom of the target as described above. A framing camera viewed this target along its axis at 6 degrees from the vertical. Eleven images of 1 ns dwell time were obtained for each of two energy cuts. The time-dependent radial temperature profiles obtained from the framing camera data normalized to the x-ray flux measured with the bolometer array and x-ray diodes are shown in Fig. 8. As can be seen from the data, the plastic/gold half-moon could not be seen through the foam on this shot. It is expected that the density of the foam was too dense for the system to be optically thin. The temperature profiles on this shot are relatively flat at each time interval. Fig. 9 shows the diameter of the tungsten sheath versus time. The tungsten sheath had an implosion velocity of 35 cm/μs during the last 5 ns of the implosion. Also shown in Fig. 9 is the brightness temperature of the hohlraum as function of time. As can be seen from Fig. 6, a peak brightness temperature of 160 ± 13 eV was reached at 539.2 ns at a diameter of 1.6 mm. However, at a diameter of 0.8 mm (while the system is still open), the brightness temperature reached 230 ± 18 eV which is the highest temperature we have ever reached in a dynamic hohlraum before final stagnation. We have plans to use this source in future static-walled hohlraum experiments.

The high-temperature dynamic hohlraum environment of the plastic annulus shot has formed the basis for our first capsule experiments on Z. For driving capsule implosions the dynamic hohlraum offers the advantage of high radiation temperatures in an open volume with reasonable symmetry. For the designer, the main constraint is the time between first-strike and stagnation when the dynamic hohlraum is open. The capsule design and z-pinch modeling are being carried out using radiation hydrodynamics code calculations. High-resolution capsule performance simulations are accomplished with 1-D calculations using experimentally obtained drive histories. Integrated 2-D simulations incorporating the tungsten wire impact on the dynamic hohlraum are used to address capsule drive symmetry. The first Z capsules are 1600 μm inner diameter spheres with 30 micron thick polystyrene shells fabricated by General Atomics. For containment of the fill gas, a permeation barrier consisting of approximately 2.5 μm of PVA is coated on the shell. These capsules are filled with 16-18 ATM of deuterium gas and 0.1 ATM of sulfur-hexafluoride for x-ray imaging diagnostics. Clean 1-D simulations predict a neutron yield of ~$3x10^{10}$ for an undoped polystyrene shell while the yield increases to ~$1x10^{11}$ with a 2.5% atomic fraction germanium doping.

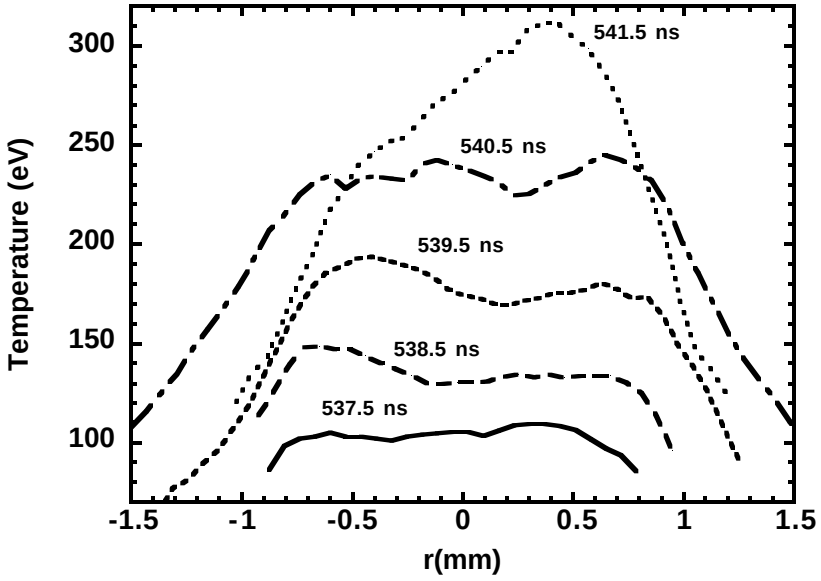

Fig. 8 Radial temperature profiles for low density foam shot.

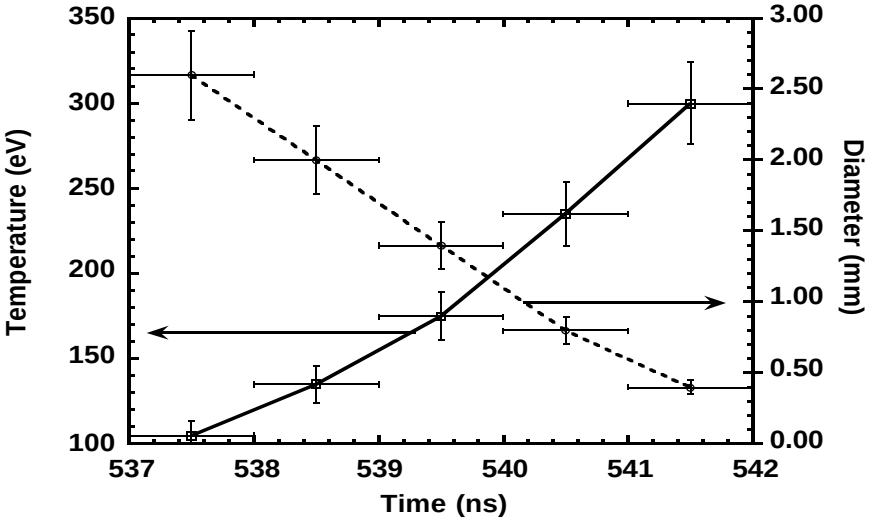

Fig. 9 Diameter and temperature versus time for low density foam target.

3.0 STATIC-WALLED HOHLRAUM CONCEPT

In order to gain preliminary understanding of the static-walled hohlraum concept and to test our numerical simulations, we have performed a series of hohlraum experiments with a single-sided drive at the 20 MA level in the SNL Z facility. This experimental configuration is shown in Figure 10. In these experiments, the hohlraums (6 mm diameter and 7 mm long) have been heated to radiation temperatures in the range of 80-100 eV. Experiments to date include investigations of the z-pinch x-ray sources, the hohlraum temperatures, the diagnostic hole closure, axial temperature gradients, pulse shaping, azimuthal symmetry, and radiation transport and plasma filling in capsule/x-ray shield configurations.

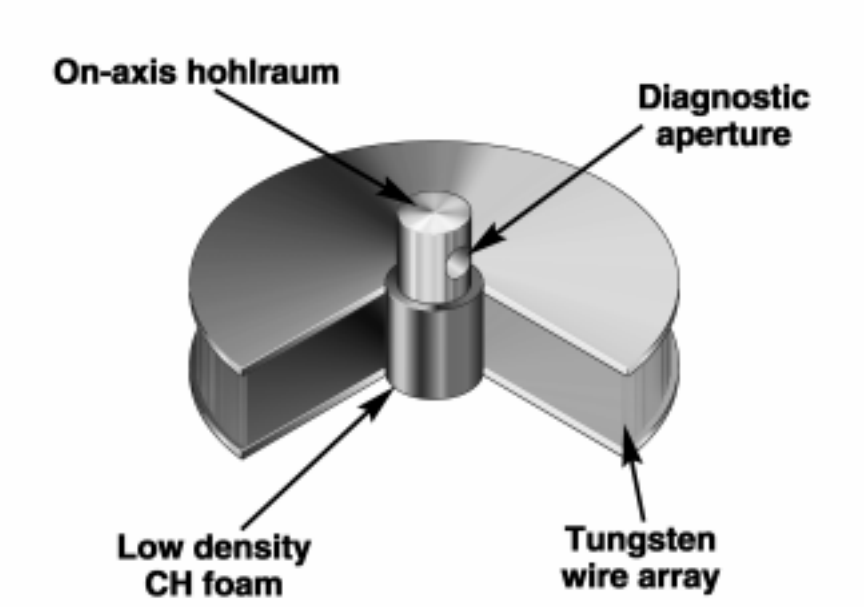

Fig. 10 Experimental arrangement for static-walled experiments.

The x-ray source for the static-walled hohlraum is investigated with an experimental arrangement in which the hohlraum in figure 10 is not included (the arrangement for x-ray source studies is similar to the dynamic hohlraum configuration of Fig. 4). The basic idea is that we first must measure the power history of the source that is used to drive the hohlraum. Characteristics of this x-ray power input are measured with an on-axis diagnostic suite that includes an array of K- and L- edge filtered photocathode detectors (referred to as XRDs), two time-resolved x-ray framing cameras, a bolometer, and a calorimeter. The central cylinder in these experiments is typically 8 mm in diameter and 10-20 mm tall. In the x-ray source experiments to date, the central cylinders have been constructed of copper or gold with wall thickness in the range of 2-4 μm. The interior region of the target is either vacuum or filled with low density (6 mg/cc to 14 mg/cc) CH foam. The limiting aperture for the x-ray power is ~2-6 mm — compatible with the radiation entrance hole of a 6 mm diameter hohlraum. Plots of x-ray source power as a function of time are shown in Fig. 11 for two types of central cylinder targets. When driven with a ~17 MA 10 mm long, 240 wire tungsten wire array, the thin-walled, 8 mm diameter Cu cylinder source provides an x-ray source that rises within about 1 ns to ~4-6 TW of x-ray power. This power level is consistent with that required for the ~80-90 eV "foot pulse" in a NIF-scale ICF hohlraum. The diameter of the central cylinder is such that the time between first strike and final stagnation is comparable to the 10-15 ns pulse length that is required for a typical ICF foot pulse. As will be described below, this type of source has been used as an x-ray drive in our characterizations of NIF-scale hohlraums at the 80-100 eV, 10-15 ns level. The higher power plots shown in Fig. 11 are related to our investigations of the peak power, final stagnation source. The peak x-ray power of a pinch stagnating on-axis, as viewed through the 5.8 mm limiting aperture, is ~20 TW. Another source shown in the figure peaks at ~12 TW when viewed through a 2 mm diameter limiting aperture. These types of high power final stagnation sources have not yet been used as an x-ray drive for a hohlraum. In order to demonstrate scaling adequate to extrapolate to ICF-relevant peak power conditions, we believe that the peak power source must still be improved by about a factor of two-to-three. These investigations are in progress.

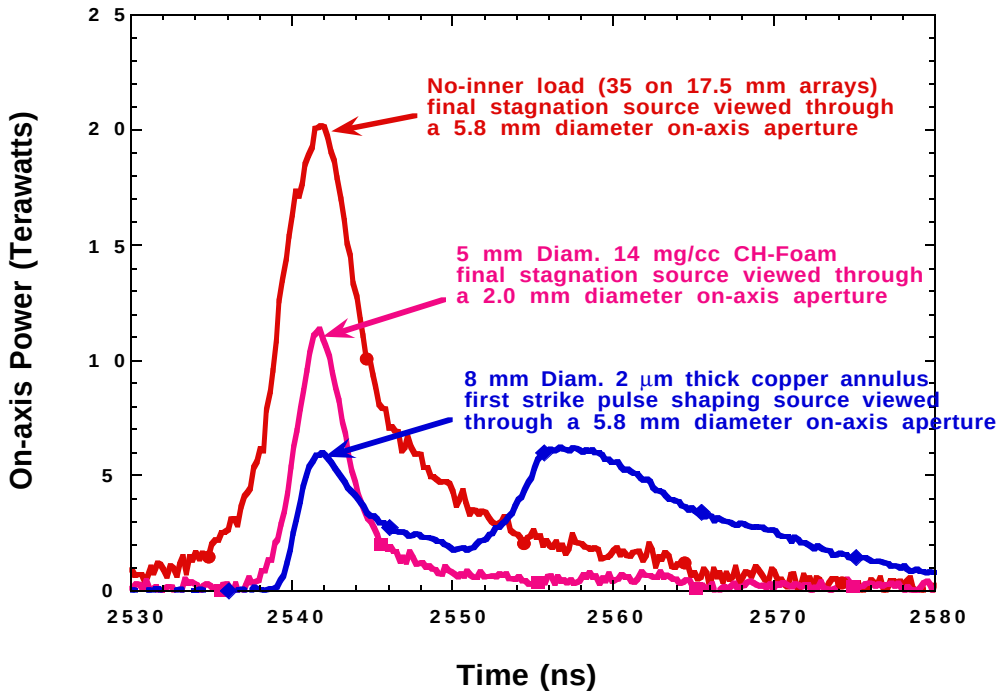

Fig. 11 Measurements of power history for first strike and final stagnation x-ray sources.

As mentioned above, the hohlraum experiments to date have used the ~4 TW power input to investigate hohlraum conditions during the ~10-15 ns foot pulse. The hohlraums are ~7 mm long and 6 mm in diameter (this is approximately the size of a NIF ignition-scale hohlraum). The

gold hohlraum walls were 25 μm thick, and the diagnostic apertures have been either 3 or 4 mm in diameter. The diagnostic aperture is viewed with an x-ray framing camera that is set up to provide 16 images — four images at 2 ns interframe time in each of four spectral cuts. Other x-ray diagnostic instruments fielded in these experiments included two arrays of K- and L- edge filtered photocathode detectors (XRDs), two transmission-grating spectrometers, a bolometer, a calorimeter, and a number of electrical power flow detectors. The filtered photocathode detector array is arranged to provide time-dependent (± 100 ps resolution) measurement of photon fluxes in spectral bands peaking at 250, 450, 800, and 1000 eV photon energies. All detectors have been calibrated with a known x-ray synchrotron source [19]. Thus, the photocathode signals together with the knowledge of hohlraum aperture size can be used to provide estimates of hohlraum radiation brightness temperature as a function of time. Such a plot is shown in Fig. 12. The vertical extent of each error bar is indicative of the spread in brightness temperatures indicated by the different detectors viewing the four different energy bands. The hohlraum temperature versus time prediction from a numerical simulation of the wire array, central cylinder, hohlraum system is also shown in the figure. It is typical for our numerical simulations to predict hohlraum radiation fields that are more intense than those indicated by the experimental measurements. This might be due to an inadequate calculational treatment of the magneto-hydrodynamic Rayleigh-Taylor instability of the imploding z-pinch, or possibly an inadequate treatment of the hydrodynamic closure of the hohlraum radiation entrance hole. We do not believe that the early-time disagreement is caused by the closure of the hohlraum diagnostic aperture. As shown in Fig. 13, images from the x-ray framing camera indicate that the diagnostic apertures remain ~80% (by area) open at the peak of the x-ray pulse.

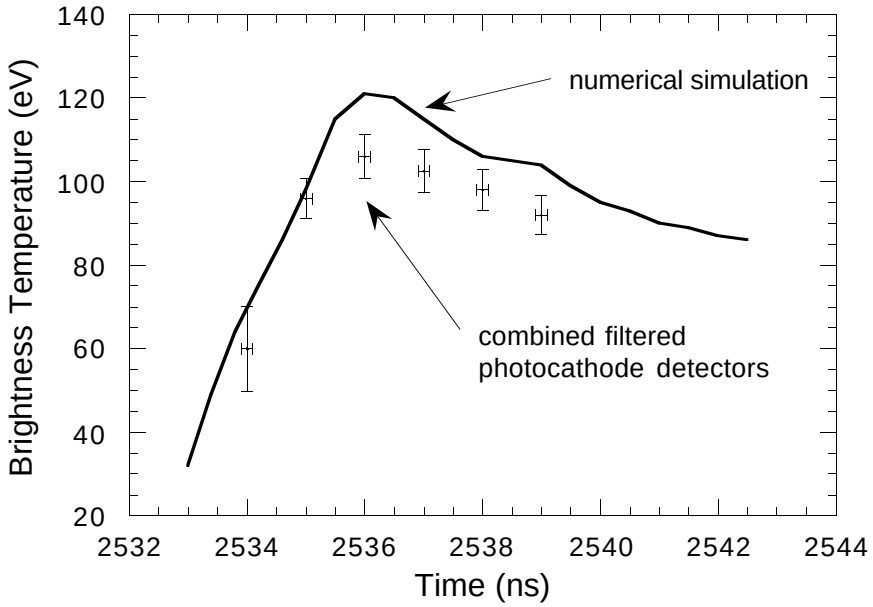

Fig. 12 Hohlraum brightness temperature versus time based on filtered photocathode detector array compared to a numerical simulation.

X-ray driven hohlraums will, by nature, have an axial gradient in the radiation field. It is anticipated that the ICF capsule symmetry effects of such gradients can be compensated for by techniques involving symmetry shields and hohlraum shaping. It is, therefore, very important that we develop an understanding of the axial temperature gradient. We have performed several hohlraum experiments relating to this issue using large, 4 mm diameter apertures in the hohlraum wall. In these experiments, the aforementioned 16 image x-ray framing camera was used to view the hohlraum wall in a time- and spectral-dependent fashion. Lineouts through the exposure-converted digitized image can then provide an indication of the variation of intensity of x-ray emission from the wall. This variation can then be normalized to the brightness temperature indicated by a comparably filtered photocathode detector. Numerical simulations indicate that the variation in the brightness temperature of the wall should vary by about 2.5-3.0 eV/mm in these

hohlraums. As shown in Fig. 14, the gradient indicated by the x-ray framing camera images is in approximate agreement with our expectations.

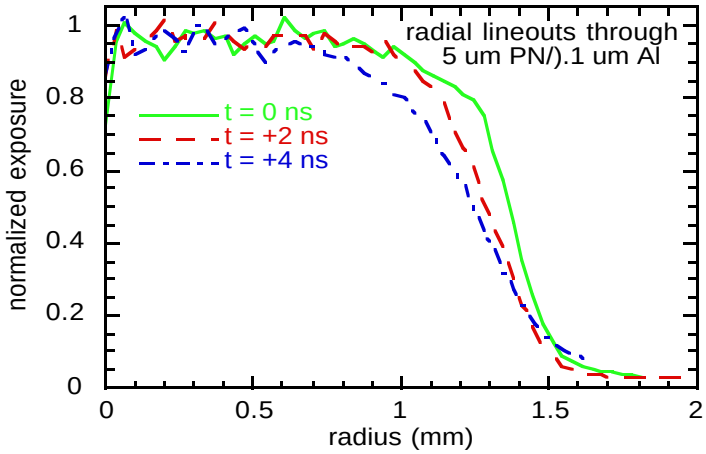

Fig. 13 Radial average lineouts of normalized exposure in x-ray framing camera images indicate that the hohlraum diagnostic apertures remain more than 50% open (by area) for up to 4 ns after the peak of the hohlraum temperature pulse.

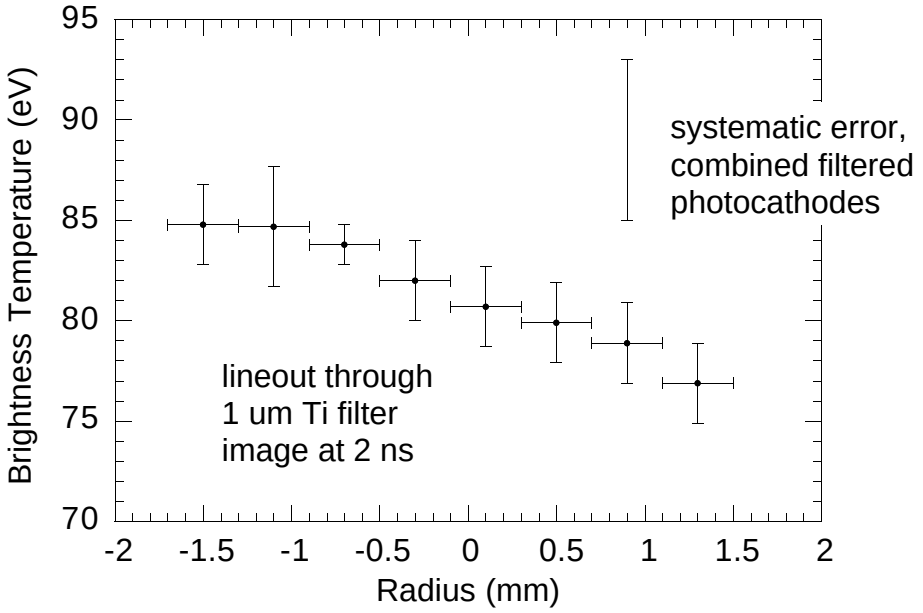

Fig. 14 Axial gradient in the hohlraum brightness temperature as indicated by a lineout through an x-ray framing camera image of the diagnostic aperture.

Our numerical simulations of the static walled hohlraum are two-dimensional and, hence, assume that the radiation field in the hohlraum will be azimuthally-symmetrical. It is important to determine the validity of this basic assumption. An experimental arrangement that we have used to measure azimuthal symmetry in the static-walled hohlraum is illustrated in Fig. 15. In this experiment, the filtered photocathode (XRD) array was used to view the east wall of the hohlraum and one of the transmission grating spectrometers (TGS) was used to view the west wall of the

hohlraum. As can be seen in the figure, the XRD and TGS channels viewing spectral bands centered at 250 eV and 450 eV overlay very well throughout the entire hohlraum power pulse. This data is very encouraging in that it does not indicate any obvious problem with azimuthal asymmetries for this type of hohlraum.

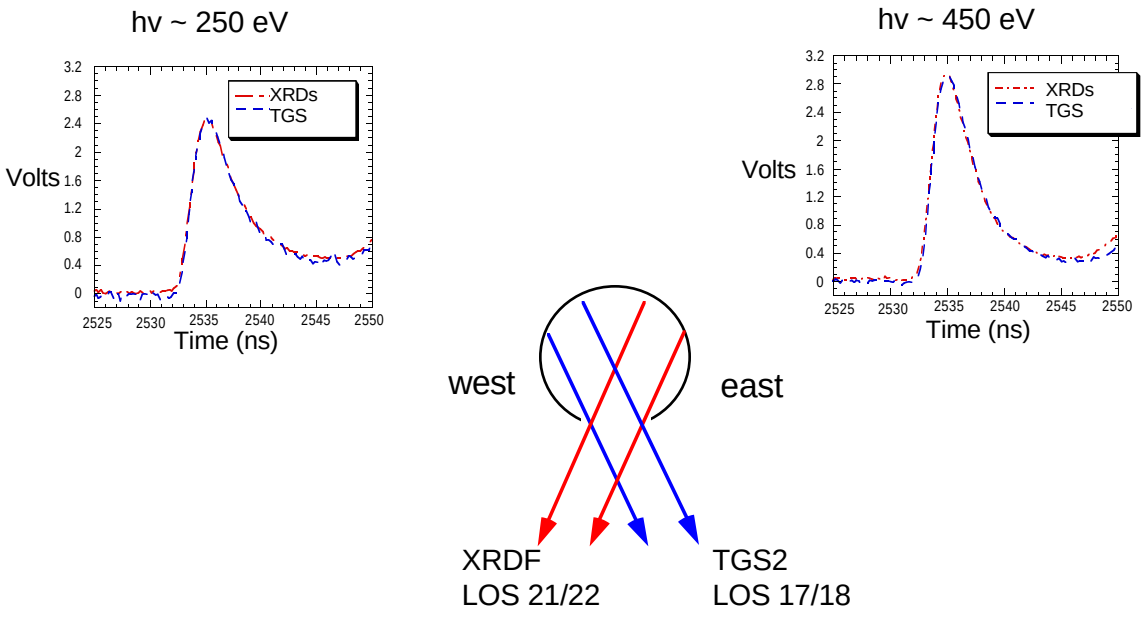

Fig. 15 Comparison of the power versus time for 250 eV and 450 eV x-rays emitted from the hohlraum diagnostic aperture at two different azimuthal viewing angles.

Two types of experiments are commonly used in the indirect-drive ICF community to learn about capsule drive symmetry — reemission ball experiments and imploded core imaging experiments. Both types of experiments require time- and energy-resolved x-ray imaging of the capsule using simultaneous polar and equatorial lines-of-sight. So far, we have done two static-wall hohlraum experiments involving x-ray shields and capsules as a first step in developing the capability for capsule symmetry experiments on Z. These experiments are illustrated in Fig. 16. Dimensions of the hohlraums, x-ray shields, and capsules used in the experiments are indicated in the drawings on the left-hand side of the figure. These were our first experiments in which we attempted to view a capsule with both polar and equatorial lines-of-sight. The polar (on-axis) views were provided by two time-resolved x-ray framing cameras. One camera was situated directly on axis and the other was at 6 degrees off-axis. The equatorial images were provided by a time-resolved x-ray framing camera placed at 12 degrees above the equator and 20 degrees offset from the aperture center. Each of the on-axis cameras provided 24 images — 11 images at 1 ns interframe time in each of the two spectral cuts and two time integrated images. The equatorial camera was set up to provide 16 images — four images at 2 ns interframe time in each of four spectral cuts. Other x-ray diagnostic instruments fielded in these experiments included three K- and L- edge filtered photocathode arrays, a transmission-grating spectrometer, two bolometers, and a calorimeter. In these experiments, we obtained self-consistent, time-dependent measurements of the radiation fields in the drive region, the hohlraum wall, and the "back side" of the x-ray shield. One of the kimfoil-filtered (hν~250 eV) axial x-ray images is shown in the upper right-hand corner of Fig. 16. The capsule, x-ray shield, shield supports, and source region (apertured by the 3 mm diameter hole in the top of the hohlraum) are evident in the image. One of the radial x-ray images (boron filter, hν~180 eV) is shown on the lower right-hand side of the viewgraph. The capsule, stalk, and interior hohlraum wall (apertured by the 3 mm diameter hole in the side of the hohlraum) are evident in the image. The 100 μm diameter Be support wires are the smallest features that can be seen in these images. These are being compared with our numerical simulations. We also gained insight into the time-dependent hohlraum hole closure and plasma filling. In particular, features of ~100-200 μm were clearly visible until ~5-10 ns into the pulse, and the diagnostic holes were "closed" at ~10 ns. The central cylinder (the x-ray source region) in the experiments was 9 mm long, 8 mm diameter, 2

μm thick Cu wall, and partially filled with CH foam. At first strike, the effective brightness temperature in the source region appears to be ~110 eV. The peak hohlraum temperatures measured in these capsule/ x-ray shield experiments were ~80-90 eV. Hole closure and plasma filling limit our ability to measure the hohlraum temperature after about 5-10 ns into the pulse. In the future, we plan to use hole tamping and low-z fill techniques to measure hohlraum temperatures further into the pulse and to explore higher temperature hohlraum environments.

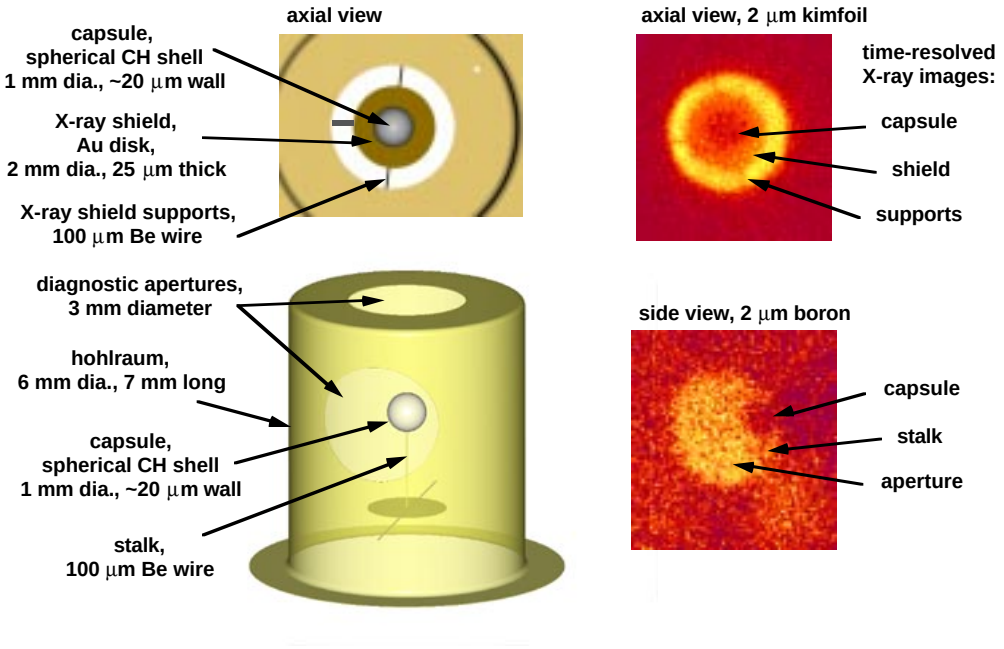

Fig. 16 Experimental arrangement and x-ray framing camera data from preliminary static-walled hohlraum experiments involving x-ray shields and spherical capsules.

4.0 Z-PINCH HOHLRAUM CONCEPT

The experimental investigation of the z-pinch driven hohlraum concept has only recently begun. We have performed experiments to optimize the radiation temperature of the z-pinch driven hohlraum by studying the coupling of electrical energy to the z-pinch plasma as a function of the A-K separation at the z-pinch load. Smaller A-K gaps decrease both the initial load inductance and the radiation losses from the hohlraum. The z-pinch load in these experiments was effectively one end of the configuration shown in Fig. 3, and represents an extension of earlier work with larger hohlraums and larger A-K gaps [20]. As the x-ray energy increases and the time-scale of the radiation drive becomes longer, it is more important to reduce radiation losses through the A-K gap. On Z, we have found that it is possible to decrease the A-K gap from 5 mm to as small as 1.5 mm with no noticeable loss in electrical coupling efficiency. Our highest temperature z-pinch driven hohlraum configuration thus far has a 1.5 mm A-K gap and uses a 10 mm long, 20 mm diameter tungsten wire array load. We measured the x-ray emission from a 12 mm^2 region of the hohlraum wall using a soft x-ray spectrometer that has a time resolution of approximately 500 psec. As shown in Fig. 17, the spectral shape of the x-ray emission from the hohlraum wall at the time of maximum x-ray power is well approximated by a 150 eV blackbody. In the future we intend to study hohlraums that have even smaller A-K gaps, since they have important implications for the maximum temperature achievable on the next generation pulsed power accelerator.

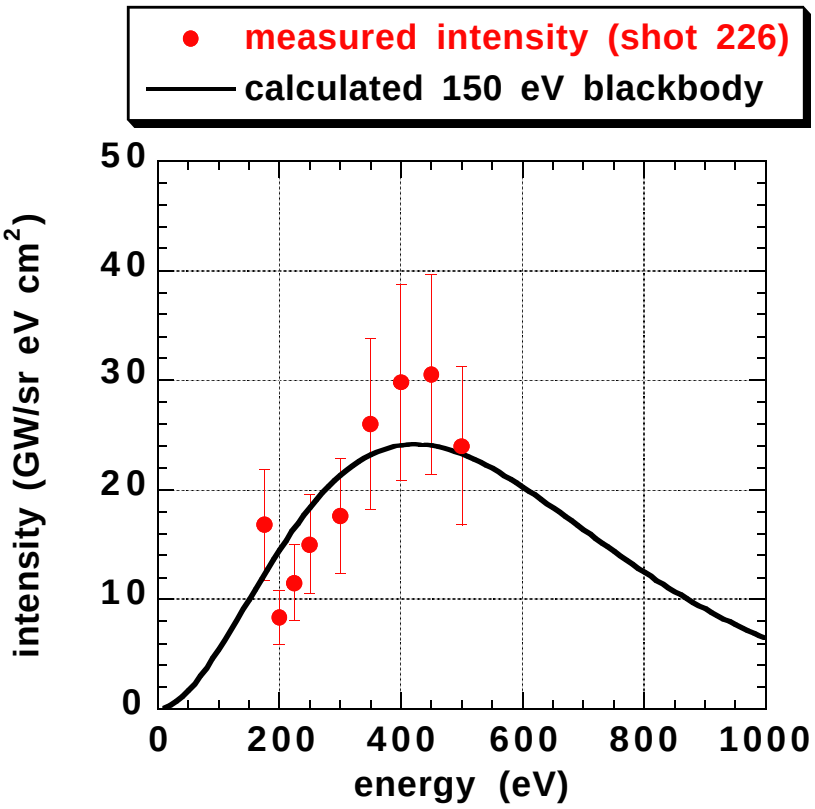

Fig. 17 The measured x-ray intensity in a z-pinch driven hohlraum compared to the x-ray intensity that would be emitted from a 150 eV Planckian.

5.0 SUMMARY

Using the Z facility at Sandia National Laboratories, three z-pinch hohlraum concepts are being investigated. Calculations indicate that at a current level of 60 MA, the dynamic hohlraum configuration is capable of driving high yield capsules to outputs of 600 MJ. To date, the dynamic hohlraum has achieved a brightness temperature of 180 ± 14 eV in an arrangement suitable for driving capsules arranged internal to this hohlraum. A temperature of 230 ± 18 eV has been achieved in a dynamic hohlraum central target configuration suitable for driving external hohlraums. Exploding pusher DD capsule experiments have recently begun using a dynamic hohlraum as an x-ray source. Static-walled hohlraum experiments include investigations of the z-pinch x-ray sources, the hohlraum temperatures, the diagnostic hole closure, axial temperature gradients, pulse shaping, azimuthal symmetry, and radiation transport and plasma filling in capsule/x-ray shield configurations. The hohlraum experiments to date have utilized pulse-shaping cylinders designed to produce a ~4 TW x-ray source and drive the hohlraum to ICF-relevant foot pulse temperatures of 80-100 eV. It is found that plasma filling and diagnostic aperture issues become significant at ~5-10 ns into the pulse. We plan to investigate hole-tamping and low density CH foam fill as techniques to mitigate these problems. Final stagnation x-ray sources have been demonstrated at the ~15 TW level. Simple scaling arguments suggest that an increase to the 30-50 TW level will be required in the 20 MA Z facility to demonstrate a reasonable extrapolation to an ICF-relevant peak hohlraum radiation temperature with a proposed 50-60 MA z-pinch driver. These investigations are in progress. Experiments to optimize the radiation temperature of the z-pinch driven hohlraum by studying the coupling of electrical energy to the z-pinch plasma as a function of the A-K separation at the z-pinch load have recently been performed. Smaller A-K gaps decrease both the initial load inductance and the radiation losses from the hohlraum. The z-pinch driven hohlraum concept will be further explored in a series of experiments on Z during the upcoming year.

REFERENCES

[1] LINDL, J. D., Phys. Plasmas ***2*** (1995) 3833.

[2] ANDERSON, O. A., BAKER, W. R., COLGATE, S. A., ISE, J., and PYLE, R. V., Phys. Rev. ***110*** (1958) 1375.

[3] SETHIAN, J. D. et al., Phys. Rev. Lett. ***59*** (1987) 892.

[4] MATZEN, M. Keith, Phys. Plasmas ***4*** (1997) 1519.

[5] MATZEN, M. K., DEENEY, C., LEEPER, R. J., PORTER, J. L., SPIELMAN, R. B. CHANDLER, G. A., DERZON, M. S., DOUGLAS, M. R., FEHL, D. L., HEBRON, D. E., NASH, T. J., OLSON, R. E., RUGGLES, L. E., SANFORD, T. W. L., SEAMEN, J. F., STRUVE, K. W., and STYGAR, W. A., to be published in Plasma Physics and Controlled Fusion, February 1999.

[6] SPIELMAN, R. B., BREEZE, S. F., DEENEY, C., DOUGLAS, M. R., LONG, F., MARTIN, T. H., MATZEN, M. K., MCDANIEL, D. H., MCGURN, J. S., NASH, T. J., PORTER, J. L., RUGGLES, L. E., SANFORD, T. W. L., SEAMEN, J. F., STYGAR, W. A., TORRES, J. A., ZAGAR, D. M., JOBE, D. O., PETERSON, D. L., SHOUP, R. W., STRUVE, K. W., MOSTROM, M., CORCORAN, P., and SMITH, I., (Proc. of the 11th Int. Conf. On Particle Beams, Prague, Czech Republic, 1996), (JUNGWIRTH, K., and ULLSCHMIED, J., Eds.), Czech Academy of Sciences, Prague (1996) 150.

[7] BLOOMQUIST, D. D., STINNETT, R. W., MCDANIEL, D. H., LEE, J. R., SHARPE, A. W., HALBLEIB, J. A., SCHLITT, L. G., SPENCE, P. W., and CORCORAN, P., (Proc. of the Sixth IEEE Pulsed Power Conf., Arlington, VA, 1997), (TURCHI, P. J., and BERNSTEIN, B. H., Eds.), IEEE, New York (1987) 310.

[8] MATZEN, M. K., HUSSEY, T. W., MONTRY, G. R., and MOREL, J. E. "A 1D Scaling Study of Radiation Sources Using Imploding Liners," submitted for deposit to the National Technical Information Service, Springfield, VA 22161.

[9] SMIRNOV, V. P., Plasma Physics and Controlled Fusion ***33*** (1991) 1697.

[10] BROWNELL, J.H., BOWERS, R. L., MCLENITHAN, K. D., and PETERSON, D. L., Phys. Plasmas ***5*** (1998) 2071.

[11] ALLSHOUSE, George, private communication (1995).

[12] OLSON, R. E., CHANDLER, G. A., DERZON, M. S., HEBRON, D. E., LASH, J. S., LEEPER, R. J., NASH, T. J., ROCHAU, G. E., SANFORD, T. W. L., ALEXANDER, N. B., GIBSON, C. R., to be published in Fusion Technology, March, 1999.

[13] HAMMER, J. H., LINDL, J. D., and TABAK, M., these Proceedings.

[14] NASH, T. J., DERZON, M. S., ALLSHOUSE, G., DEENEY, C., SEAMEN, J. F., MCGURN, J., JOBE, D., GILLILAND, T., MACFARLANE, J. J., WANG, P., PETERSON, D. L., (Proc. of the 4th Int. Conf. on Dense Z-Pinches, Vancouver, Canada, 1997), (PEREIRA, N. R., DAVIS, J., and PULSIFER, P. E., Eds.), American Institute of Physics, AIP Confernce Proceedings 409, Woodbury, New York (1997) 175.

[15] DERZON, M. S., ALLSHOUSE, G. O., DEENEY, C., LEEPER, R. J., NASH, T. J., MATUSKA, W., PETERSON, D. L., MACFARLANE, J. J., RYUTOV, D. D., Sandia National Laboratories Report SAND98-1190, Albuquerque (1998).

[16] NASH, T. J., DERZON, M. S., CHANDLER, G. A., LEEPER, R. J., FEHL, D., SEAMEN, J., MCGURN, J., LAZIER, S., TORRES, J., JOBE, D., GILLILAND, T., HURST, M., MOCK, R., MCKENNEY, J., HEBRON, D., ALBERTS, T., MACFARLANE, J. J., PETERSEN, D., BOWERS, R., MATUSKA, W., RYUTOV, D. D., to be published in Physics of Plasmas, 1999.

[17] NASH, T. J., DERZON, M. S., CHANDLER, G. A., FEHL, D., LEEPER, R. J., HURST, M., JOBE, D., TORRES, J., SEAMEN, J., LAZIER, S., GILLILAND, T., MCGURN, J., accepted for publication in Review of Scientific Instruments, Volume 70, Number 1, January, 1999.

[18] HURST, M. J., NASH, T. J., DERZON, M. S., KELLOGG, J. W., TORRES, J. A., MCGURN, J., SEAMEN, J., JOBE, D., LAZIER, S. E., accepted for publication in Review of Scientific Instruments, Volume 70, Number 1, January, 1999.

[19] CHANDLER, G. A., DEENEY, C., CUNEO, M., FEHL, D. L., MCGURN, J.S., MCKENNEY, J. L., MILLS, J., SPIELMAN, R. B., STRUVE, K. W., TORRES, J.A., accepted for publication in Review of Scientific Instruments, Volume 70, Number 1, January, 1999.

[20] PORTER, John L., Bull. Am. Phys. Soc. ***42*** (1997) 1948.